Coherent Transfer of Light Polarization to Electron Spins in a Semiconductor

Hideo Kosaka,[1,2] Hideki Shigyou,[1] Yasuyoshi Mitsumori,[1,2] Yoshiaki Rikitake,[2,3] Hiroshi Imamura,[3,2] Takeshi Kutsuwa,[2] Koichiro Arai,[2,4] and Keiichi Edamatsu[1]

[1]*Laboratory for Nanoelectronics and Spintronics, Research Institute of Electrical Communication, Tohoku University, Sendai 980-8577, Japan*

[2]*CREST-JST, Saitama 332-0012, Japan*

[3]*Nanotechnology Research Institute, AIST, Tsukuba 305-8568, Japan*

[4]*ERATO Semiconductor Spintronics Project, JST, Saitama 332-0012, Japan*

(Received 20 October 2007; published 7 March 2008)

We demonstrate that the superposition of light polarization states is coherently transferred to electron spins in a semiconductor quantum well. By using time-resolved Kerr rotation, we observe the initial phase of Larmor precession of electron spins whose coherence is transferred from light. To break the electron-hole spin entanglement, we utilized the big discrepancy between the transverse g factors of electrons and light-holes. The result encourages us to make a quantum media converter between flying photon qubits and stationary electron-spin qubits in semiconductors.

DOI: 10.1103/PhysRevLett.100.096602 PACS numbers: 72.25.Fe, 78.67.−n, 85.35.Ds

None of the physical implementations of quantum bits or qubits is suitable for all aspects of quantum-information technology. Quantum-information interfaces [1,2] connecting those qubits are thus needed to place the right qubit at the right position. Photons are the natural messenger qubits for fast and reliable communication [3], whereas electron spins in a semiconductor are suitable processor qubits for stable and scalable computation [4–6]. Quantum media conversion (QMC) between the photon qubit and the electron-spin qubit will drastically extend the potential of quantum-information and -communication technologies.

Quantum coherence is one of the essential features of quantum phenomena and is a central issue in quantum-information technology. Researchers exploring the feasibility of semiconductor-based quantum computation have demonstrated that not only the optical dipole coherence of excitons [7,8], but also electron-spin coherence can be controlled optically [9–13] and electrically [5,6]. The electron-spin coherence time, or transverse spin-relaxation time T_2^*, is generally much longer than the optical dipole coherence time and could be further prolonged by storing the electron-spin coherence in a nuclear spin [14]. On the other hand, researchers exploring the feasibility of semiconductor-based quantum communication have shown that triggered single photons [15,16] and polarization-entangled photon pairs [17–20] can also be generated in semiconductors. One of the remaining challenges in developing all-semiconductor quantum-information and -communication devices is to transfer the quantum coherence of the superposition state of a photon (based on polarization degree of freedom) to that of an electron in a semiconductor (based on spin degree of freedom). Although the physics of optical orientation has a long history [21], little attention has been paid to the coherent transfer of the polarization state of light to electron spins.

In this Letter, we demonstrate for the first time coherent transfer of light polarization to electron spins. We not only show the projective up and down spin states or spin population as reported before [22–25] but also show that in a V-shaped three-level system with Voigt geometry an arbitrary coherent superposition state can be transferred from light polarization to electron spins. Although we used classical light and a spin ensemble, this coherent transfer is the first demonstration of the conditions needed for transferring the quantum state [26–28] of a photon to an electron.

We begin by summarizing the operating principle of our QMC scheme (Fig. 1). Any light polarization state is represented by a state vector, called a Stokes vector, in the Poincaré sphere (PS) spanned by the basis vectors $|\sigma^+\rangle$ and $|\sigma^-\rangle$, corresponding to right and left circular polarizations. In the same manner, any electron-spin state is represented by a Bloch vector in the Bloch sphere (BS) spanned by the basis vectors $|\uparrow\rangle_e$ and $|\downarrow\rangle_e$, corresponding to up and down spin polarizations. Both the PS and BS thus are the equivalent special unitary group, SU(2) Hilbert spaces connected via selection rules. The selection rules for a light-hole (LH) exciton are given by $|\sigma^+\rangle \rightarrow |\uparrow\rangle_e \otimes |\downarrow\rangle_{\mathrm{LH}}$ and $|\sigma^-\rangle \rightarrow -|\downarrow\rangle_e \otimes |\uparrow\rangle_{\mathrm{LH}}$ [21]. An arbitrary light polarization state $\alpha|\sigma^+\rangle + \beta|\sigma^-\rangle$ is thus transferred to the exciton spin state $\alpha|\uparrow\rangle_e \otimes |\downarrow\rangle_{\mathrm{LH}} - \beta|\downarrow\rangle_e \otimes |\uparrow\rangle_{\mathrm{LH}}$, where the electron-spin state is entangled with the hole spin state. The coherence time of a hole spin, however, is so short that the entangled electron spin might be instantly converted into incoherent mixture of spin states projected along the z axis, and an incoherent mixture cannot be used as a qubit. The problem can be solved by applying an in-plane (transverse) magnetic field B_x to configure the V-shaped three-level system shown in Fig. 1(b). The magnetic field lifts the Kramer's degeneracy of the LH and reconfigures the eigenstates as $|\pm x\rangle_{\mathrm{LH}} = |\downarrow\rangle_{\mathrm{LH}} \pm |\uparrow\rangle_{\mathrm{LH}}$ while keeping the degeneracy of the electron with the smaller g factor. Via

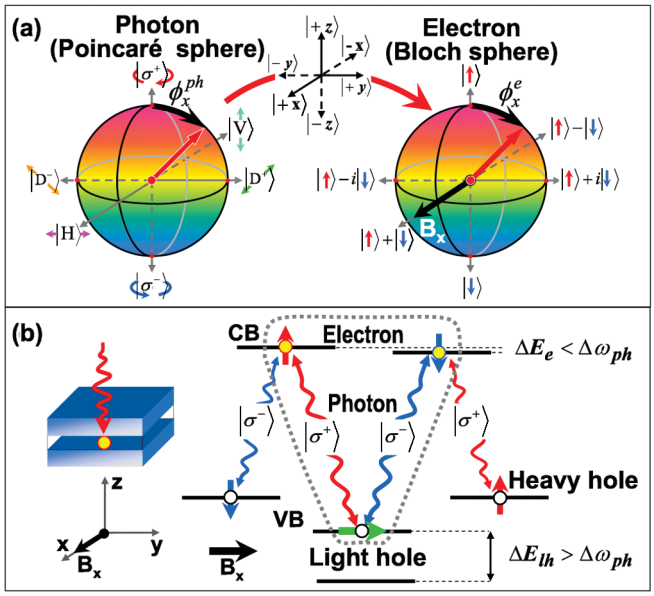

FIG. 1 (color). The operating principle of our QMC scheme from photon polarization to electron-spin polarization. (a) State vectors representing a photon polarization in a Poincaré sphere and an electron-spin polarization in a Bloch sphere with the phase definitions used in Fig. 3. (b) Schematic diagrams of the experimental setup and the relevant energy levels together with optical spin selection rules under an in-plane magnetic field B_x that forms a V-shaped three-level system consisting of a degenerate electron state and one eigenstate of nondegenerate light-hole (LH) states. The photon bandwidth ($\Delta\omega_{\mathrm{ph}}$) should be larger than the electron Zeeman splitting (ΔE_e) but smaller than the LH Zeeman splitting (ΔE_{LH}).

the resonant transition between the $|-x\rangle_{\mathrm{LH}}$ state and the degenerated electron states, the same selection rules lead to the transition from $\alpha|\sigma^+\rangle + \beta|\sigma^-\rangle$ to $(\alpha|\uparrow\rangle_e + \beta|\downarrow\rangle_e) \otimes |-x\rangle_{\mathrm{LH}}$. Since the transferred electron-spin state is not entangled with the LH state, its coherence time is not limited by the short LH spin coherence time or the fast relaxation to the ground heavy-hole (HH) state. This is the key point of our QMC scheme. It is essential to use the LH states since we cannot sufficiently lift the Kramer's degeneracy of the HH state by applying an in-plane magnetic field because of the very small transverse g factor [29]. The electron coherence time is limited by the electron-hole exchange interaction, which can be greatly extended by extracting a hole while leaving an electron in a quantum well [9] or a quantum dot [24,30].

The sample we used contained a high-quality 11 nm-thick undoped GaAs quantum well embedded in undoped $Al_{0.3}Ga_{0.7}As$ grown by molecular beam epitaxy on a semi-insulating GaAs substrate with the growth interruption to have a high quality well. The photoluminescence (PL) spectrum of the HH exciton shown in Fig. 2(a) has three structures that correspond to the different confinement energies caused by the one-monolayer fluctuation of the well width. The homogeneous linewidth should be much narrower than the inhomogeneous linewidth of 1 nm (2 meV). The photoluminescence excitation (PLE) spectrum in Fig. 2(a) shows that the LH exciton is energetically well separated from the HH exciton. The quantum well was designed to have a relatively small electron transverse g factor ($g_{e,\perp} = -0.21$) and a relatively large LH transverse g factor ($g_{\mathrm{LH},\perp} = -3.5$) under the in-plane magnetic field B_x used to configure the V-shaped three-level system. The g factors were calculated using the $\mathbf{k}\cdot\mathbf{p}$ method [31,32] and those absolute values were confirmed by the Kerr and PLE measurements. We chose the nonzero g factor for an electron intentionally in order to be able to observe the initial phase of the spin precession under a moderate B_x. A mode-locked Ti:sapphire laser (Coherent MIRA 900) delivering 130 fs pulses at a repetition rate of 76 MHz was used to pump and probe the sample through a wavelength-tunable filter consisting of a diffraction grating (FWHM = 0.38 nm) in each path and a variable delay line in only the probe path. All the measurements were made at 5 K and at normal incidence in the Voigt geometry [Fig. 1(b)]. The electron-spin dynamics free from the influence of the dynamic nuclear-spin polarization [13,14] was extracted by periodically switching the polarization of the pump light between two orthogonal states. The pump power dependence of the typical Kerr rotation signals [Fig. 2(b)] is linear up to 1 mW, which corresponds to the exciton density of 5×10^9 cm^{-2} or an average exciton spacing of 160 nm, which is much greater than the exciton Bohr radius (12 nm). Below this power level, all the temporal responses were unchanged. All the measurements in the work reported here were made in this linear range where created excitons were well separated from each other.

Quantum spin coherence of an electron is often indicated by the Larmor precession or the quantum beats [9,12,22,23], which is usually visualized by time-resolved Kerr rotation measurements [9,10]. Although the Kerr rotation provides information only about the spin projection or population along the growth axis, we can infer the spin orientation of the superposition state from the initial phase of the spin precession. Here, we show how the inferred initial phase of the generated electron spin is related to the pump-light polarization. We first selected six light polarization states [$|\sigma^+\rangle$, $|\sigma^-\rangle$, $|D^+\rangle$, $|D^-\rangle$ ($\pm 45°$ degree polarization), and $|H\rangle$, $|V\rangle$ (horizontal and vertical polarization, respectively)] and measured the temporal evolution of the Kerr rotation angle θ_K under $B_x = 7$ T [Fig. 2(c)]. The lower-energy side of the LH exciton peak ($\lambda_E = 796.2$ nm) was excited with one of the above-mentioned polarizations and probed at $\lambda_P = 795.7$ nm with the H polarization [Fig. 2(a)]. Four of the states perpendicular to the x axis ($|\sigma^+\rangle$, $|D^+\rangle$, $|\sigma^-\rangle$, and $|D^-\rangle$) provided approximately the same amplitude, while the phases were sequentially shifted by the angle of $\pi/2$. These results suggest that the $|D^-\rangle$ states, which are coherent superpositions of $|\sigma^+\rangle$ and $|\sigma^-\rangle$ states $|\sigma^+\rangle \pm i|\sigma^-\rangle$, create equivalent superpositions of the $|\uparrow\rangle_e$ and $|\downarrow\rangle_e$ states $|\uparrow\rangle_e \pm i|\downarrow\rangle_e$ (normalization omitted for brevity).

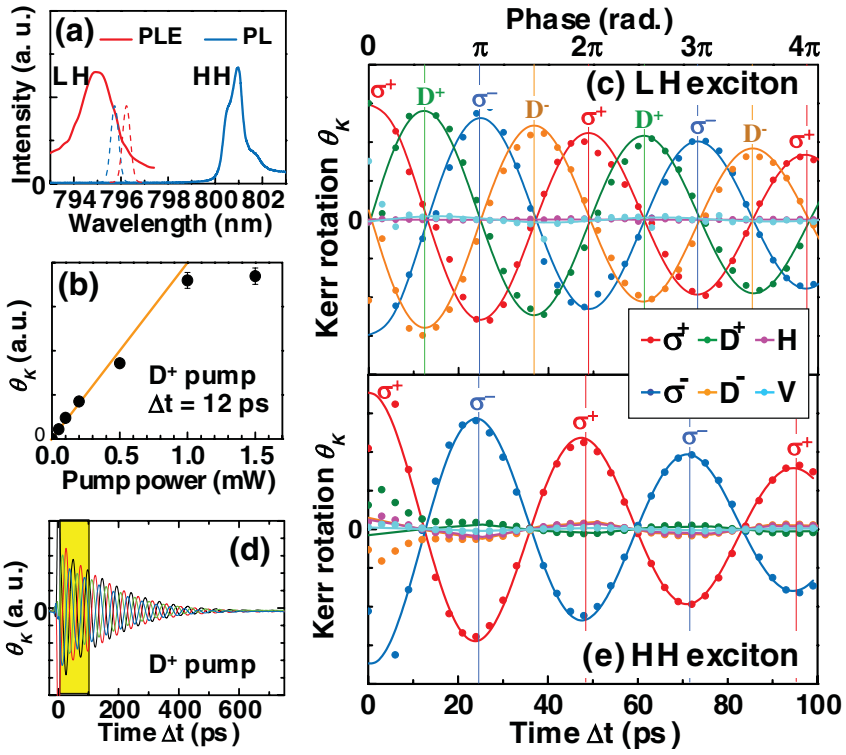

FIG. 2 (color). (a) PL (blue) and PLE (red) spectra detected at HH exciton emission under $B_x = 7$ T. The broken lines show the spectra of the pump (red) and probe (blue) lights. (b) Pump power dependence of the Kerr rotation angle (θ_K) with D^+ under $B_x = 7$ T at $\Delta t = 12$ ps. Error bars show standard deviation. (c) Temporal evolution of θ_K with six basis polarizations under $B_x = 7$ T. Each of the consecutive phase shifts in the cyclic order of $|\sigma^+\rangle$ (red) $\rightarrow |D^+\rangle$ (green) $\rightarrow |\sigma^-\rangle$ (blue) $\rightarrow |D^-\rangle$ (orange) $\rightarrow |\sigma^+\rangle$ in $\pi/2$ steps coincides well with that of electron-spin states expected from the pump-light polarizations. In contrast, excitation with the $|H\rangle$ (pink) and $|V\rangle$ (sky blue) polarization, which correspond to the B_x direction, generate negligible signals. (d) Large-time-scale view of Fig. 2(c). (e) HH-excitation case for comparison. Only $|\sigma^{\pm}\rangle$ excitations generate relatively large signals, indicating that spins are always projected along the z axis.

It is natural that the states along the x axis ($|H\rangle$ and $|V\rangle$) provided negligible amplitude because those state vectors are parallel to the field. From the decay of precession amplitude seen in Fig. 2(d), the T_2^* is estimated to be 160 ps. In contrast to the LH excitation, the HH excitation ($\lambda_E = \lambda_P = 800.8$ nm) gave the conventional result [Fig. 2(e)], where the $\sigma^{\pm}$ pump corresponding to the projected states $|\uparrow/\downarrow\rangle_e$ provided significant amplitude but the others did not. The lack of the amplitude seen with D^+ and D^- pumping indicates that superposition of the $|\uparrow\rangle_e$ and $|\downarrow\rangle_e$ states could not be created by the HH excitation. We verified the one-to-one correspondence between the light polarization phase φ_x^{ph} and the electron-spin phase φ_x^e as shown in Fig. 3. The phases φ_x^e and φ_x^{ph} are, respectively, the angles of the state vectors in the PS and the BS, such that $|D^+\rangle = \cos(\varphi_x^{\mathrm{ph}}/2)|\sigma^+\rangle + i\sin(\varphi_x^{\mathrm{ph}}/2)|\sigma^-\rangle (\varphi_x^{\mathrm{ph}} = \pi/2)$ as shown in Fig. 1(a). The electron phases φ_x^e inferred from the peaks well coincide with the pump-light phases φ_x^{ph}. This coincidence is evidence of coherent polarization transfer.

To show the role of the lift of the hole state Kramer's degeneracy induced by the in-plane magnetic field, we measured B_x-field dependence of θ_K with the D^+ polarization [Fig. 4(a)]. The times to reach maximum and minimum signals are well reproduced by the theoretical calculations shown by the dashed curves. The first maximum points are delayed by $\pi/2$ for all B_x as in Fig. 2(c). Note that as the magnetic field decreases, the precession amplitude decreases much faster than T_2^*, indicating that the electron-spin coherence is gradually lost through the entanglement with the degenerated hole spin as in the HH case. Although the exchange interaction between the electron and the LH in $|-x\rangle_{\mathrm{LH}}$ state might act as an additional effective magnetic field along the x axis, as in the case of HH [22], it is not remarkable because of the fast LH relaxation to the HH. The distinguishability of the LH states is demonstrated in Fig. 4(b), where the θ_K is measured at $\Delta t = 12$ ps ($\pi/2$ phase) with the D^+ polarization at $B_x = 7$ T is plotted against both the pump and probe wavelengths. The splitting of the peaks along the pump wavelength originates from the LH Zeeman splitting. The

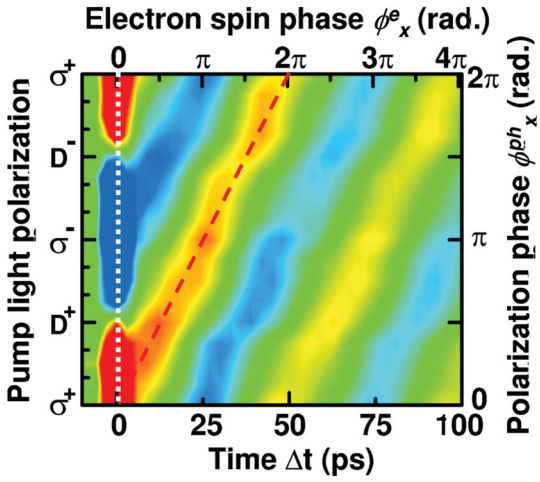

FIG. 3 (color). Time evolution of θ_K as a function of pump-light polarization under $B_x = 7$ T. The linear streak pattern indicates coincidence of the phase angle of the electron spins φ_x^e to that of the light polarization φ_x^{ph}. Definitions of the phases are shown in Fig. 1(a).

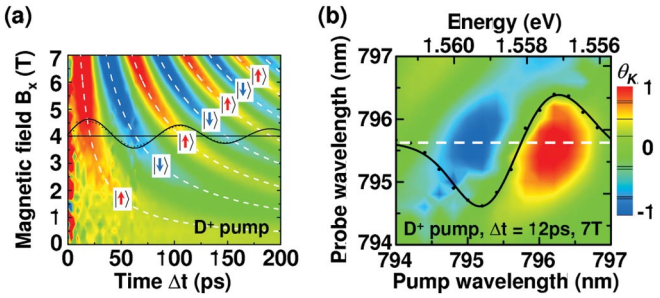

FIG. 4 (color). (a) Time evolution of θ_K as a function of B_x with D^+ pumping. The cut of θ_K at $B_x = 4$ is shown by the dots fitted to a damped sine function. The dashed curves are the calculated tracks of the $B_x - \Delta t$ values needed to detect electrons aligned to $|\pm z\rangle_e$ when an electron transverse g factor of -0.21 is assumed. (b) θ_K as a function of pump/probe wavelengths with D^+ at $\Delta t = 12$ ps under $B_x = 7$ T. Dots show the pump spectrum of θ_K at the probe wavelength used for all the LH measurements (795.7 nm) with a curve fitted by a two-component Gaussian.

low (high)-energy peak showing the positive (negative) sign corresponds to the LH spin state $|\pm x\rangle_{\mathrm{LH}} = |\uparrow\rangle_{\mathrm{LH}} \pm |\downarrow\rangle_{\mathrm{LH}}$, where the pump-light polarization state $|D^+\rangle$ is transferred to the electron-spin state $|\pm y\rangle_e = |\uparrow\rangle_e \pm i|\downarrow\rangle_e$, respectively. The pump and probe wavelengths in the above experiments were chosen to have the peak signal. We can fit the pump spectrum of θ_K (dots) at a fixed probe wavelength by using two Gaussian functions with a separation given by the calculated transverse LH g factor of -3.5 (solid curve). This well-separated spectrum is not observed in the HH-excitation case, where because of the Kramer's degeneracy, only one peak is observed with any polarization of pump light.

The coherent polarization transfer demonstrated here is essentially different from the previously demonstrated coherent electron-spin controls based on an optical Stark effect [10], spin-flip Raman scattering [11], or Rabi oscillation [12], each of which needs intense light as a driving force defined and is therefore not suitable for transferring the phase state of a single photon. Our QMC scheme is not limited to the transfer of a single-particle state but can be generalized to the transfer of a two-particle state or an entangled state, which is the kind of transfer needed for quantum repeaters [33,34] or routers for scalable quantum communication and distributed quantum computation. Although the wavelength used here is about half of the telecom wavelength, QMC between photons of different wavelengths by a nonlinear up-conversion process has been shown to be possible [2]. The transfer of light polarization only in the y-z plane in the PS as shown here is sufficient for implementation of a quantum repeater based on the Bennett-Brassard 1984 cryptographic scheme [2,3] by converting the time-bin phase coding to the polarization coding.

In conclusion, we have demonstrated coherent polarization transfer from light to electron spins in a semiconductor. From the phase of spin precession, we inferred the initial phase that should correspond to the phase of light polarization. The electron-hole spin entanglement was broken by the big discrepancy between the g factor of the electron and the g factor of the light hole. Although we have demonstrated only a necessary condition of QMC, this is a step toward the realization of all-semiconductor quantum interfaces between a photon and an electron spin.

We are grateful to Professors Hideo Ohno, Toshihide Takagahara, Keiji Ono, and Jaw-Shen Tsai for fruitful discussions. This work was supported in part by the SCOPE program (No. 41402001) of MIC Japan, a grant from MEXT Japan (No. 16710061), and a grant from NEDO Japan.

[1] R. Vrijen and E. Yablonovitch, Physica E (Amsterdam) **10**, 569 (2001).
[2] S. Tanzilli *et al.*, Nature (London) **437**, 116 (2005).
[3] C. H. Bennett and G. Brassard, in *Proc. of Int. Conf. on Computers, Systems and Signal Processing* (IEEE, New York, 1984), p. 175.
[4] D. Loss and D. P. DiVincenzo, Phys. Rev. A **57**, 120 (1998).
[5] J. R. Petta *et al.*, Science **309**, 2180 (2005).
[6] F. H. L. Koppens *et al.*, Nature (London) **442**, 766 (2006).
[7] N. H. Bonadeo *et al.*, Science **282**, 1473 (1998).
[8] A. Zrenner *et al.*, Nature (London) **418**, 612 (2002).
[9] J. M. Kikkawa and D. D. Awschalom, Nature (London) **397**, 139 (1999).
[10] J. A. Gupta *et al.*, Science **292**, 2458 (2001).
[11] M. V. G. Dutt *et al.*, Phys. Rev. Lett. **94**, 227403 (2005).
[12] A. Greilich *et al.*, Phys. Rev. Lett. **96**, 227401 (2006).
[13] M. Atatüre *et al.*, Science **312**, 551 (2006).
[14] M. V. G. Dutt *et al.*, Science **316**, 1312 (2007).
[15] C. Santori *et al.*, Phys. Rev. Lett. **86**, 1502 (2001).
[16] Z. Yuan *et al.*, Science **295**, 102 (2002).
[17] K. Edamatsu *et al.*, Nature (London) **431**, 167 (2004).
[18] R. M. Stevenson *et al.*, Nature (London) **439**, 179 (2006).
[19] N. Akopian *et al.*, Phys. Rev. Lett. **96**, 130501 (2006).
[20] G. Oohata, R. Shimizu, and K. Edamatsu, Phys. Rev. Lett. **98**, 140503 (2007).
[21] *Optical Orientation*, edited by F. Meier and B. P. Zakharchenya (Elsevier, Amsterdam, 1984).
[22] T. Amand *et al.*, Phys. Rev. Lett. **78**, 1355 (1997).
[23] A. P. Heberle, W. W. Ruhle, and K. Ploog, Phys. Rev. Lett. **72**, 3887 (1994).
[24] M. Kroutvar *et al.*, Nature (London) **432**, 81 (2004).
[25] H. Kosaka *et al.*, Appl. Phys. Lett. **90**, 113511 (2007).
[26] J. I. Cirac *et al.*, Phys. Rev. Lett. **78**, 3221 (1997).
[27] D. N. Matsukevich and A. Kuzmich, Science **306**, 663 (2004).
[28] J. F. Sherson *et al.*, Nature (London) **443**, 557 (2006).
[29] X. Marie *et al.*, Phys. Rev. B **60**, 5811 (1999).
[30] H. Kosaka *et al.*, Phys. Rev. B **67**, 045104 (2003).
[31] E. L. Ivchenko and A. A. Kiselev, Sov. Phys. Semicond. **26**, 827 (1992).
[32] P. Le Jeune *et al.*, Semicond. Sci. Technol. **12**, 380 (1997).
[33] H.-J. Briegel *et al.*, Phys. Rev. Lett. **81**, 5932 (1998).
[34] P. van Loock *et al.*, Phys. Rev. Lett. **96**, 240501 (2006).